

1                   **Inconsistent urbanization effects on summer precipitation**  
2                   **over the typical climate regions in central and eastern China**

3  
4                   Fan Xiao<sup>1,2,3</sup>, Bin Zhu<sup>1,2,3,\*</sup>, Tong Zhu<sup>4</sup>

5                   1Collaborative Innovation Centre on Forecast and Evaluation of Meteorological Disasters, Nanjing University of I  
6                   nformation Science & Technology, Nanjing, China

7                   2Key Laboratory of Meteorological Disaster, Ministry of Education (KLME), Nanjing University of Information S  
8                   cience & Technology, Nanjing, China

9                   3Special Test Field of National Integrated Meteorological Observation, Nanjing University of Information Science  
10                   & Technology, Nanjing, China

11                   4IM System Group, Inc. @NOAA/NESDIS/STAR, College Park, Maryland, USA

12  
13                   *Abstract:* Using 30-year data (1983-2012) from 428 stations, we study summer precipitation differences  
14                   between urban and rural areas in 5 Chinese climate regions: the Pearl River Delta (PRD), the Middle and  
15                   Upper reaches of the Yangtze River (MUYR), the Yangtze River Delta (YRD), the North China Plain  
16                   (NCP), and Northeast China (NEC). By analyzing heavy rain (HR) (24 h precipitation $\geq$ 100 mm) and  
17                   light rain (LR) (0.1 mm $\leq$ 24 h precipitation $\leq$ 25 mm), we find that urbanization has had inconsistent  
18                   effects on precipitation. Higher HR occurs over urban areas of the PRD and YRD than rural areas, and  
19                   lower HR occurs over urban areas of the MUYR, NCP and NEC than rural areas. The urban LR is less  
20                   than the rural LR in all climate regions. The correlation between precipitation and the convective  
21                   available potential energy (CAPE) or humidity explains the regional differences in urbanization effects  
22                   on HR. HR is greatly affected by the CAPE in the PRD and YRD, where the CAPE is high ( $>600$  J/kg at  
23                   14:00 LT), water vapor is abundant ( $>45$  kg/m<sup>2</sup> at 14:00 LT), and the urban heat island increases the  
24                   urban HR. However, HR is greatly affected by humidity in the MUYR, NCP and NEC, where the CAPE  
25                   and water vapor are less ( $\leq500$  J/kg and  $\leq40$  kg/m<sup>2</sup> at 14:00 LT) and the urban HR is mainly suppressed  
26                   by the urban dry island. Our results indicate that urbanization promotes HR in wet climates but suppresses  
27                   HR in dry climates during summer in central and eastern China.

28                   *Keywords:* different climate zones, precipitation of different intensities, inconsistent urbanization effects  
29                   on precipitation, physical mechanism

30                   **Introduction**

31                   Over the past 30 years, China has experienced rapid urbanization. A series of environmental  
32                   variations, such as underlying surface replacement, population surges, and pollution emissions, have  
33                   changed the physical and chemical properties of the urban atmosphere, and these variations have complex  
34                   impacts on meteorological factors, such as temperature, humidity, and precipitation (Yang et al. 2011[49];  
35                   Hao et al. 2013[14]; Song et al. 2014[43]; Han et al. 2014[13]; Li et al. 2016[25]). Researchers have  
36                   suggested that the impacts of urbanization on precipitation mainly originated from three factors (Baik et  
37                   al. 2001[2]; Rozoff et al. 2003[39]; Baik et al. 2007[3]): urban heat island (UHI) effects (Olfe and Lee  
38                   1971[35]; Changnon 1979[5]; Baik 1992[1]; Bornstein and Lin 2000[4]; Kaufmann et al. 2007[21]; Han  
39                   and Baik 2008[12]; Lin et al. 2011[30]; Li et al. 2011a[24];

40                   \* Corresponding author at: Collaborative Innovation Centre on Forecast and Evaluation of Meteorological  
41                   Disasters, Nanjing University of Information Science & Technology, Nanjing, China.

42 E-mail address: binzhu@nuist.edu.cn (B. Zhu).

43 Wang et al. 2015[46]; Liang et al. 2017[28]), underlying surface changes (such as urban dry island (UDI)  
44 effects caused by decreases of low-layer atmospheric humidity) (Zhang et al. 2009[51]; Kishtawal et al.  
45 2010[22]; Miao et al. 2011[31]; Souma et al. 2013[44]; Wu and Tang 2015[47]; Zhou et al. 2015[54])  
46 and aerosol emissions (Houze 1993[16]; Pruppacher and Klett 1997[40]; Rosenfeld et al.  
47 2000[37]; Zhang et al. 2009[51]; Li et al. 2011b[26]; Guo et al. 2014b[9]; Li et al. 2019[27]).

48 The impacts of urbanization on precipitation vary regionally as revealed by previous studies; thus,  
49 it is often difficult to determine the dominant factors of urbanization effects due to the joint effects of  
50 local geography and climatic background (Han et al. 2014[13]; Li et al. 2016[25]). Some researchers  
51 agreed that urbanization enhances precipitation (Changnon et al. 1979[5]; Baik et al. 2001[2]; Mote et  
52 al. 2007[32]; Zhang et al. 2010[52]; Lin et al. 2011[30]; Li et al. 2011a[24]; Wang et al. 2015[46]; Liang  
53 et al. 2017[28]); some suggested that urbanization suppresses precipitation (Kaufmann et al. 2007[21];  
54 Zhang et al. 2009[51]; Wu and Tang 2015[47]; Zhou et al. 2015[54]); while others suggested that  
55 urbanization showed no obvious effects on precipitation (Tayan 1997[45]). Generally, the UHI is caused  
56 directly by urbanization and referring to the phenomenon that the temperature of city is higher than that  
57 of the surrounding suburban or rural areas (Oke 1973[34]), and it affects precipitation by changing the  
58 urban thermodynamic field (Han et al. 2014[13]). The UHI reduces the stability of the atmospheric layer  
59 by forming heat island circulation, which is conducive to trigger convection and form convective  
60 precipitation, and then affects the distribution of precipitation over cities and their downstream areas  
61 (Olfe and Lee 1971[35]; Baik 1992[1]; Han and Baik 2008[12]). As early as the 1970s, METROMEX  
62 confirmed the urbanization effect of increasing rainfalls through 5-year intensive observations and found  
63 that precipitation within 50 to 75 km of the St. Louis city core and its downwind areas increased by 25%  
64 compared with the background areas (Changnon et al. 1979[5]). Lin (2011)[30] suggested that the UHI  
65 has strengthened precipitation in Taipei and its downwind areas and affected the time and location of  
66 rainfall systems. Similarly, some studies in China agreed that urbanization has led to increases of  
67 convective precipitation over many places, such as the urban agglomerations of the Pearl River Delta  
68 (PRD) (Li et al. 2011a[24]), the city core of Shanghai (Liang et al. 2017[28]), and the city lower reaches  
69 of Beijing (Wang et al. 2015[46]).

70 However, the inhibitory urbanization effects on precipitation have been found in some studies  
71 (Kaufmann et al. 2007[21]; Zhang et al. 2009[51]; Wu and Tang 2015[47]; Zhou et al. 2015[54]). The  
72 UHI increases the temperature of the urban boundary layer and lifts the cloud base height, which  
73 lengthens the raindrop falling path, resulting in the evaporation of light raindrops. In addition, the  
74 decreasing atmospheric water vapor supplied by urban surfaces is also a possible reason for the decrease  
75 of urban light rain (Kaufmann et al. 2007[21]). Urban undersurfaces, which are mostly replaced by  
76 artificial surfaces, such as concrete, have weaker water permeability, higher thermal conductivity and  
77 lower heat capacity than natural surfaces (Shem and Shepherd 2009[42]), causes UDI effects, which  
78 suppress urban precipitation (Zhang et al. 2009[51]). The urbanization processes in the Yangtze River  
79 Delta (YRD) (Wu and Tang 2015[47]), the PRD, and the Beijing-Tianjin-Hebei (Zhou et al. 2015[54])  
80 expand the surface impervious areas, leading to reductions in surface evaporation and local atmospheric  
81 moisture, thereby decreasing summer precipitation.

82 A large amount of gaseous pollutants and aerosols are emitted during urban production and life, and  
83 some of them act as cloud condensation nuclei (CCNs), which participate in microphysical processes  
84 and cloud precipitation processes or affect precipitation through radiation effects of scattering and  
85 absorption (Han et al. 2014[13]). The aerosol effect on precipitation is highly uncertain and related to  
86 aerosol size, quantity, chemical composition, cloud type, precipitation type, climatic and geographical

87 conditions and other factors (Houze 1993[16]; Pruppacher and Klett 1997[40]; Li et al. 2019[27]). The  
88 long-term simulation results of Zhang et al. (2010)[52] showed that aerosols in the YRD increase the  
89 water vapor mixing ratio of the urban boundary layer and cause significant enhancement of urban  
90 precipitation.

91 Under the combined influences of the above factors (such as the UHI, aerosol, underlying surface),  
92 the effects of urbanization on precipitation becomes uncertain. Some scholars believed that whether  
93 urbanization increases (Mote et al. 2007[32]), triggers (Baik et al. 2001[2]) or decreases (Zhang et al.  
94 2009[51]) precipitation depends on the relative importance of various factors (Baik et al. 2001[2]; Han  
95 et al. 2014[13]; Wang et al. 2015[46]; Li et al. 2016[25]) related to the scale of the city and its surrounding  
96 geographic features. For example, in the early stage of urbanization, the UHI plays a dominant role in  
97 the enhancement of precipitation in a city. As the water supply of the underlying surface continues to  
98 decrease, the inhibition of urbanization on precipitation will gradually increase, which will offset some  
99 of the UHI enhancement to precipitation (Wang et al. 2015[46]). Other scholars have proposed that  
100 urbanization increases the surface roughness, which reduces the surface wind speed and results in the  
101 convergence of near-surface wind fields (Baik et al. 2001[2]). When considering the aerosol effects on  
102 precipitation, on the one hand, it increases the retention time of cloud droplets in air and promotes the  
103 condensation growth of cloud droplets, thus enhancing precipitation; while on the other hand, its  
104 absorption effect of radiation can warm the atmosphere and cool the surface, which makes the  
105 atmospheric stratification more stable, resulting in an opposite effect on the precipitation as compared  
106 with the UHI (Han et al. 2014[13]).

107 The above studies have shown urbanization impacts on local precipitation, and these studies mostly  
108 focused on one single city or city cluster over one region (Shastri et al. 2015[41]), with few  
109 comprehensive studies investigating different intensities of precipitation over different climate regions.  
110 Due to regional variations in the main contributors that affect precipitation, the dominant factors in  
111 different climate regions are still poorly understood. However, the classification of urban and rural sites  
112 is a significant cornerstone when researching urbanization impacts on precipitation. Formerly, station  
113 classification was based on single data types, such as population (Hua et al. 2008[17]), land type (Yang  
114 et al. 2013[50]), gross domestic product (GDP) (Guo et al. 2016[11]), night light (Yan et al. 2019[48]),  
115 and impervious surface area (ISA) (He et al. 2017[15]). Considering that our research areas are relatively  
116 large, including central and eastern China, we combine data observed by satellite, such as night light,  
117 population, ISA and GDP, and other aspects to define urban stations and rural stations. Based on the  
118 differences between urban and rural meteorological and climatic factors (such as the UHI, UDI,  
119 convective instability energy, water vapor content, dew-point deficit, and so on), we explore the  
120 inconsistent urbanization impacts on precipitation between urban and rural areas over different climate  
121 regions. This analysis can provide a deeper understanding of the responses of different intensities of  
122 summer rainfall to urbanization and scientific bases for assessments of local urbanization impacts on  
123 precipitation in various climates.

## 124 **1 Data and methods**

### 125 **1.1 Data**

126 The main data set employed in this article is the daily observation data set after quality control  
127 provided by the National Meteorological Information Center of China, including 2 m atmospheric

128 temperature (TEM), relative humidity (RH), visibility (VIS), and daily precipitation (P). The time span  
129 of these data includes summers from 1983 to 2012 (June, July and August). The rainfall data were  
130 recorded every hour, while other data were recorded four times per day (02:00, 08:00, 14:00, and 20:00  
131 LT). The data source is <http://data.cma.cn/en>.

132 The China gridded population dataset in km (Population Grid China) provides population data for  
133 2010. The data spatial resolution is 1 km, and it can be obtained from the Global Change Science  
134 Research Data Publishing System <http://www.geodoi.ac.cn>.

135 The Defense Meteorological Satellite Program/Operational Line-scan System (DMSP/OLS)  
136 provides ISA data for 2000, GDP data for 2006, and night light data for 2010. The spatial resolution is  
137 30 arc sec (approximately 1 km). The ISA data range from 0 to 100%, and the night light data range from  
138 0 to 63. The data source is <https://www.ngdc.noaa.gov/eog/dmsp.html>.

139 The data on the convective available potential energy (CAPE), 2 m dew-point deficit, and total  
140 column water vapor are derived from the European Center for Medium-Range Weather Forecasts  
141 (ECMWF/ERA-Interim), with a spatial resolution of 0.125° and time period from 1983 to 2012 (only  
142 including June, July and August). The data source is <https://apps.ecmwf.int/datasets/data/interim-full->  
143 [daily/levtype=sfc/](https://apps.ecmwf.int/datasets/data/interim-full-daily/levtype=sfc/).

## 144 1.2 Study region

145 The research regions in this paper are mainly distributed in central and eastern China, and five  
146 different climatic regions are selected as representative regions. As shown in Fig. 1, from south to north,  
147 the five different climatic regions are as follows: the PRD, belonging to the south subtropical marine  
148 zone; the Middle and Upper reaches of the Yangtze River (MUYR), belonging to the subtropical zone of  
149 the continent; the YRD, belonging to the northern subtropical marine zone; the North China Plain (NCP,  
150 belonging to the warm temperate zone; and Northeast China (NEC, belonging to the moderate temperate  
151 zone). The PRD is one of the three major urban agglomerations with the largest population and the  
152 strongest economic strength in south China. The Yangtze River is the largest river in Asia, and the MUYR  
153 is close to the Tibet-plateau and the local topography is complex, which includes the Sichuan Basin and  
154 mountains, thus forming a complex local climate. Moreover, this area has the largest population in  
155 western China, with its gross national product accounting for 36% of the total for China. Its downstream  
156 area (YRD) is the alluvial plain before the Yangtze River enters the sea. The YRD city cluster is one of  
157 the six internationally recognized world-class city clusters and the largest economic zone in China. The  
158 NCP is the largest and most dynamic region in the northern part of China, and it is the location of the  
159 national capital city. The NEC region has vast mountains and rich forests, and its total amount of forest  
160 storage accounts for about one third of the total in China. Each area has their own unique climate type  
161 and urbanization process.

162 According to Fig. 1a, precipitation and CAPE are distinctive in five climatic zones and generally  
163 decrease from south to north, and they are larger in the PRD and YRD than in the MUYR, NCP and NEC,  
164 with the CAPE of NEC particularly low.

## 165 1.3 Station classification

166 Considering that one single variable cannot reflect the degree of urbanization well, here, we use a  
167 combined dataset of four different types to divide urban and rural sites. He et al. (2017)[15] found that  
168 different ISA values show different impacts on the ecological environment. In their study, when the ISA

169 was within [1%, 10%), the ecology suffered a slight urbanization impact; when the ISA was within [10%,  
170 25%), the urbanization impact became obvious; when the ISA exceeded 25%, the ecological environment  
171 began to degrade. Therefore, grids where the meteorological station is located as the center grid are  
172 selected. If the ISA is at least in one grid among the center grid and its surrounding eight grids exceeds  
173 10%, then this station is regarded as a city station, and if at least one grid of the ISA exceeds 25%, then  
174 it is regarded as a large city station. Based on the ISA, we found that 33% of the stations (2420 in total)  
175 fit the city station condition and 21% of the city stations fit the large city station condition. Because the  
176 ISA can only represent differences of underlying surface between urban and rural areas, which may lead  
177 to inaccurate station type identifications, we added night light, GDP and population data to obtain a more  
178 accurate judgement of urban and rural stations. Considering that the selection region range of night light  
179 data for one station cannot be too large or too small (Yan et al. 2019[48]), we calculate the average night  
180 lights, GDP and population in the square with a side length of 7 km ( $7 \times 7$  grids) centered on each station.  
181 To weaken the influence of altitude in this study, the altitude difference of selected stations with the  
182 median altitude of each province is controlled within 200 m. If a station meets the altitude requirements  
183 and its sequence is in the top 33% of total stations determined by two of the four types of data (population,  
184 night light, ISA and GDP), it is classified as a city station. Similarly, if its sequence is in the top 21% of  
185 city stations, it is classified as a large city station. For city stations, except large city stations, the rest are  
186 small-medium city stations. Among the nonurban stations that meet the altitude requirements, rural  
187 stations are selected based on the "Technical Requirements for the Selection of National Reference  
188 Climate Station Sites" (Guo 2014a[8]) and the characteristics of persistent and stable location during the  
189 study period.

190 In this study, the five regions we selected are more urbanized and have 428 stations in total,  
191 including 104 large city stations, 283 small-medium city stations, and 41 rural stations. The numbers of  
192 sites per station type in the five climate regions are listed in parentheses as follows: PRD (22, 47, 8),  
193 MUYR (8, 46, 10), YRD (34, 42, 4), NCP (31, 107, 11), NEC (9, 41, 8). The distributions and  
194 classifications of stations are shown in Fig. 1b.

## 195 1.4 Precipitation classification

196 According to the national 24 h precipitation level standard of China (GB/T28592-2012),  
197 precipitation is divided into six levels (Table 1). A single precipitation event has an amount of more than  
198 0.1 mm and a duration of more than 1 h. The 24 h rainfall amount ( $y$  in mm) of a single precipitation  
199 event is converted according to the duration ( $tx$  in h) of the actual precipitation amount ( $x$  in mm) from  
200 Formula 1, and then the precipitation is classified based on  $y$  (Table 1).

$$201 \quad \frac{x}{tx} = \frac{y}{24} \rightarrow x \times \frac{24}{tx} = y \quad (1)$$

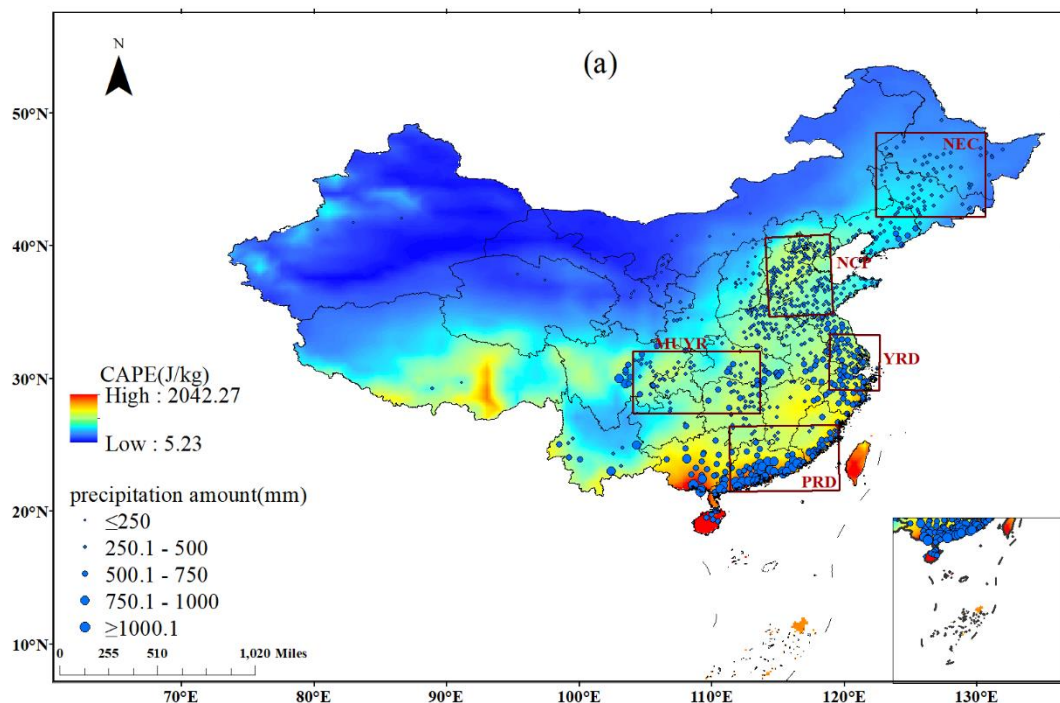
202 Table 1 Precipitation level division

range	rank	name
$0.1 \leq y \leq 9.9$ mm	1	LR: Light Rain
$10.0 \leq y \leq 24.9$ mm	2	
$25 \leq y \leq 49.9$ mm	3	
$50.0 \leq y \leq 99.9$ mm	4	
$100 \leq y \leq 249.9$ mm	5	HR: Heavy Rain
$250 \text{ mm} < y$	6	

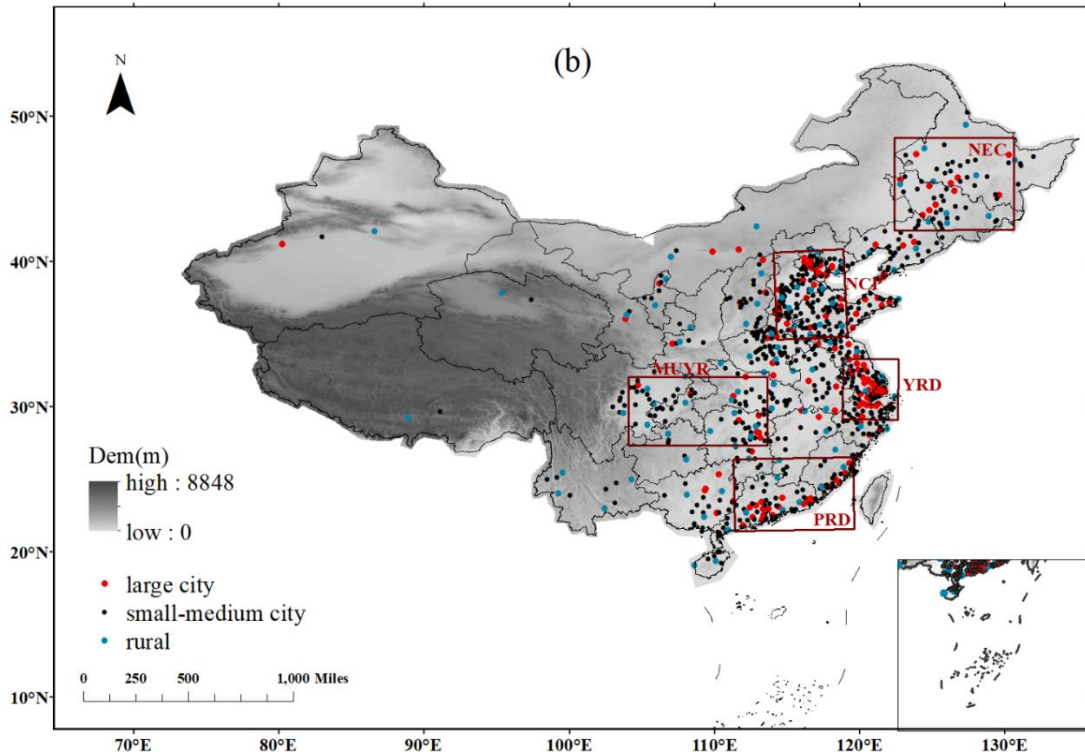
203

204 1.5 Other data processing methods

205 The differences calculation method between urban and rural physical quantity (precipitation,  
206 temperature, RH) involves subtracting the value of rural stations from that of urban stations. To avoid  
207 the bias caused by one single rural station, we did not use the method of calculating the differences  
208 between the nearest urban and rural stations. Here, we select the average value of rural stations with  
209 altitude differences of less than 100 m from the target urban station in the same region as the rural value  
210 corresponding to the target urban stations in each region. This method also minimizes the impact of  
211 altitude on physical quantity differences between urban and rural stations.



212



213

214

215 Fig. 1 (a) Distributions of summer average precipitation and CAPE; (b) elevation distributions and station  
 216 locations and types. Blue circles indicate precipitation, colored blocks indicate CAPE, red dots represent large city  
 217 stations, black dots represent small-medium city stations, blue dots represent rural stations, and red squares  
 218 represent the five different climate regions from south to north: PRD (77 stations), MUYR (64 stations), YRD (80  
 stations), NCP (149 stations), and NEC (58 stations)

## 219 2 Results and discussion

### 220 2.1 Differences in precipitation between urban and rural areas

#### 221 2.1.1 Long-term temporal variations

222 Fig. 2 shows the annual variations in six different levels of precipitation (based on GB/T28592-  
 223 2012) during the summers of 1983-2012 over urban and rural stations. The durations, counts, and  
 224 amounts of precipitation differences between urban and rural stations exhibit similar results. Levels 1 to  
 225 3 of precipitation over rural stations are significantly higher than those over urban stations, and the  
 226 precipitation differences between large cities and small-medium cities are small. The precipitation  
 227 differences at level 4 between urban and rural stations are small, and levels 5 to 6 of precipitation over  
 228 urban stations are higher than those over rural stations. Because the differences between urban and rural  
 229 stations in three precipitation characteristics in Fig. 2 are similar, subsequent studies only selected the  
 230 precipitation amounts for analysis. Fig. 3 shows the 30-year mean precipitation differences among the  
 231 three station types and is consistent with the results shown in Fig. 2, among which the amounts of urban-  
 232 rural precipitation differences are more obvious. Urbanization effects are inconsistent for different  
 233 intensities of precipitation, and they inhibit weak precipitation (levels 1-3) and weakly promote strong  
 234 precipitation (levels 4-6). However, as the intensity of precipitation increased in levels 5 and 6, the

enhancement effects of urbanization on precipitation became obvious, which can be seen from the significant differences represented by P values in Fig. 3 (one-way analysis of variance (ANOVA), with a smaller P value indicating more significant differences). To more clearly study the differences in various intensities of precipitation, levels 1 to 2 of precipitation are collectively referred to as LR (LR: Light Rain) while levels 5 to 6 of precipitation are collectively referred to as HR (HR: Heavy Rain). In particular, the precipitation in transition states (levels 3-4) has been excluded. The urban-rural differences in LR amounts and durations have passed the 95% significance test, although the urban-rural differences in HR are nonsignificant. Only when the precipitation intensity reaches the highest level and the urban size is large are the HR differences between urban and rural significant.

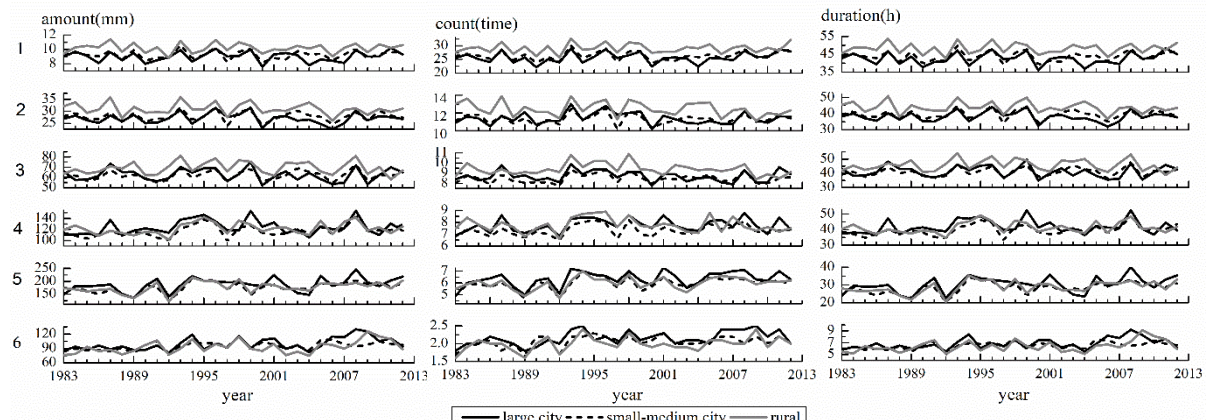


Fig. 2 Annual changes in precipitation counts, amounts, and durations of different levels over urban and rural stations. Numbers 1 to 6 represent six diverse levels of precipitation (Table 1); black solid lines represent large city stations, black dotted lines represent small-medium city stations, and gray solid lines represent rural stations

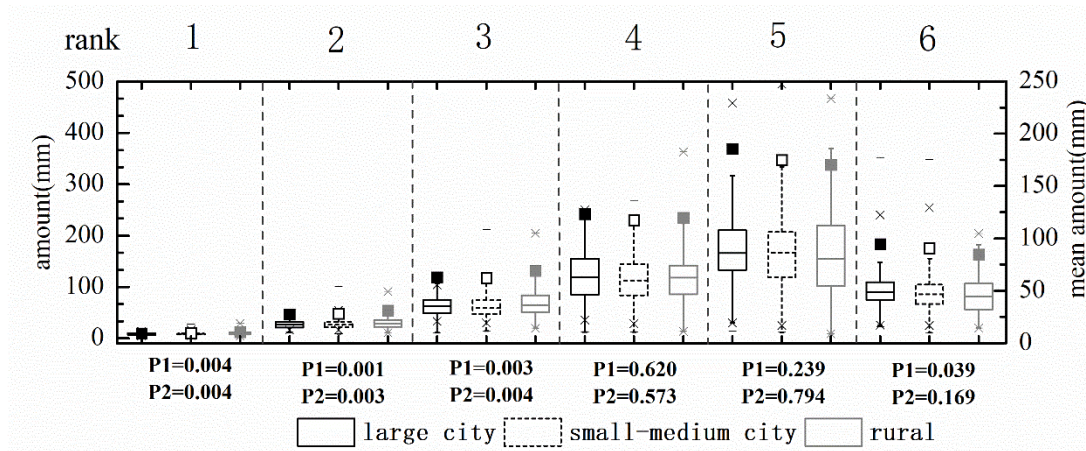


Fig. 3 Annual average precipitation amounts of different levels at urban and rural stations. Numbers 1-6 represent six diverse levels of precipitation (Table 1). The left vertical axis is the precipitation value corresponding to the box plot, and the right vertical axis is the average precipitation value corresponding to the point plot. Please note that the 2 vertical axes are in different ranges. The black solid box represents large cities, the black dotted box represents small-medium cities, the gray solid box represents rural stations, the square points are mean values, the black solid square points are mean values of large cities, the black dotted square points are mean values of small-medium cities, and the gray solid square points are mean values of rural. The upper and lower frame boundaries are the upper and lower quartiles, the upper and lower horizontal lines are the upper and lower limits, and  $\times$  is the abnormal value. P1 is the significance of the difference between large cities and rural stations, and P2 is the

258

significance of the difference between small-medium cities and rural stations

259

## 2.1.2 Diurnal variations

260

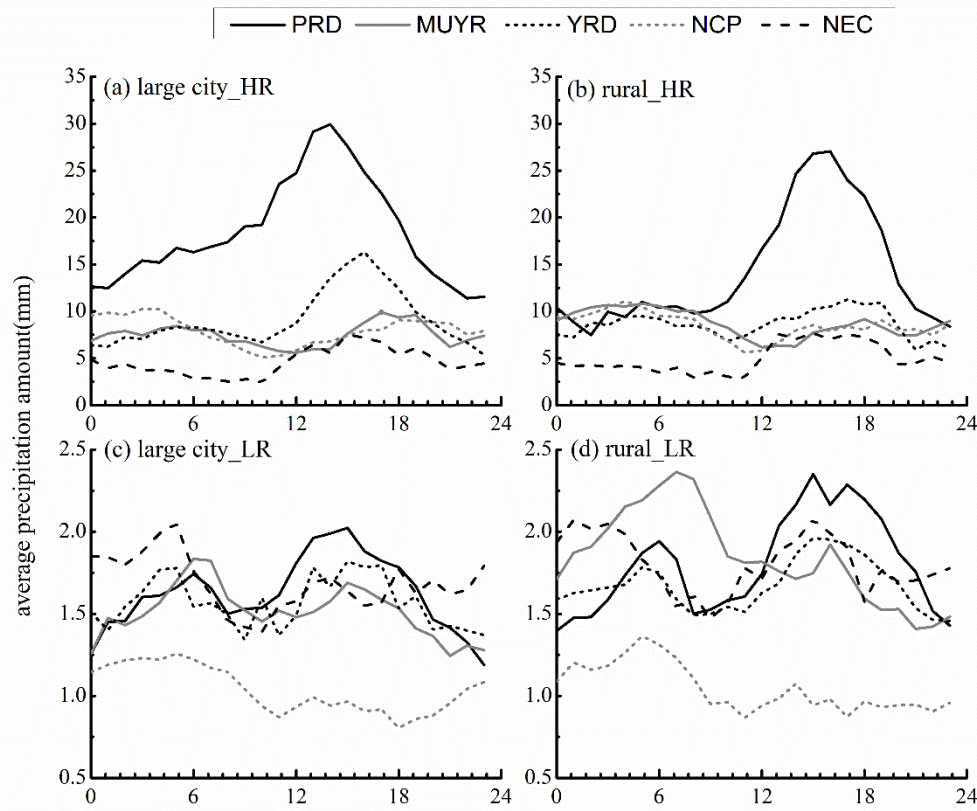
Fig. 4 shows the diurnal variation characteristics of the 30-year summer average precipitation amounts. The diurnal distributions of precipitation vary for different intensities. LR is the "double peak" type, and HR is the "single peak" type. The diurnal distributions of urban and rural stations are basically identical, although the afternoon peak of urban HR is slightly earlier than that of rural, which may be related to that ability of the UHI to trigger precipitation formation. Previous observations and numerical simulation studies demonstrated that UHIs induce convergence zones and then initiate storms (Bornstein and Lin 2000[4]; Baik et al. 2001[2]; Rozoff et al. 2003[39]).

267

Urbanization effects do not alter the diurnal variations in precipitation. Thus, because temperature and humidity present diurnal variations, precipitation may be connected to the local temperature and humidity environment; therefore, the existence of the UHIs and UDIs may cause precipitation differences between urban and rural areas.

271

Some previous studies found that urbanization would delay urban HR (Rosenfeld et al. 1999[36]; Rosenfeld et al. 2008[38]). Rosenfeld et al. (1999)[36] indicated that under the condition of insufficient water vapor, urbanization may inhibit the precipitation and delay the occurrence time of urban precipitation. In areas with sufficient water vapor, Ntelekos et al. (2009)[33] found that precipitation will increase with increases of aerosol. To investigate the delay effect, we analyzed the time series of the peak of HR starting time over the PRD and YRD regions during the 30 years. However, only a small delay signal was observed (not shown) and the fitted trend did not pass the 90% significance test. The urban aerosol effect on precipitation is complex, and urban aerosol can not only participate in the precipitation process as a CCN but also affect the precipitation process through radiation and other effects. In this study, an analysis on the effect of aerosols was not performed. Additional studies are needed to investigate the combined impacts of the UHI and increased urban aerosols on precipitation under urbanization.

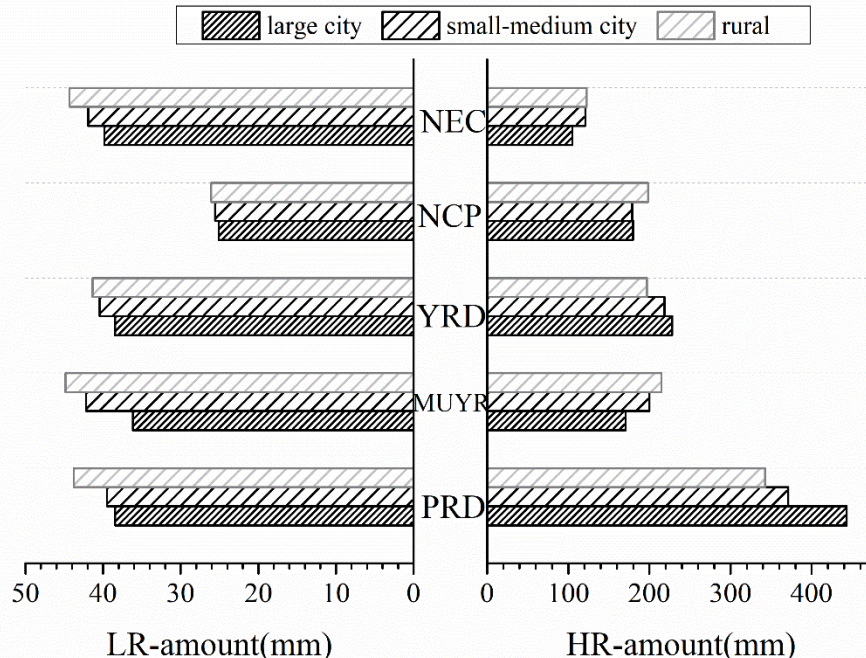


282

283 Fig. 4 Diurnal variations in annual precipitation amounts per station in summer. (a) HR over large city stations, (b)  
 284 HR over rural stations, (c) LR over large city stations, and (d) LR over rural stations. The horizontal axis  
 285 represents the local time, and the vertical axis indicates the number of precipitation events

286 **2.1.3 Regional disparities**

287 Fig. 5 shows the LR and HR differences between urban and rural areas over five typical climate  
 288 regions. It is found that the precipitation differences between urban and rural areas vary regionally.  
 289 Especially for HR, the precipitation differences over the urban stations of the PRD and YRD are higher  
 290 than those over rural stations while those over the urban stations of the MUYR, NCP and NEC are lower  
 291 than those over rural stations. The results of urban-rural precipitation differences in the PRD, YRD and  
 292 NCP also revealed by previous studies (Li et al. 2011a[24]; Jiang et al. 2016[19]; Wang et al. 2015[46];  
 293 Liang et al. 2017[28]), while less research has been performed in the MUYD and NEC. Although the  
 294 city scales and development levels of the PRD, YRD and NCP are close to each other, the NCP shows  
 295 different urbanization effects of HR. The urbanization impacts on HR may be related to the regional  
 296 climate background. Shastri et al. (2015)[41] found that urbanization impacts on heavy precipitation have  
 297 regional characteristics in India; therefore, some of the driving factors affecting HR in different climate  
 298 regions may differ, which would lead to regional disparities in HR differences between urban and rural  
 299 areas. However, the LR distributions in Fig. 5 are higher over rural areas than urban areas in all regions,  
 300 indicating that the urbanization impacts on LR are dominated by inhibitory effects, which is consistent  
 301 with previous studies showing that stratiform cloud precipitation is primarily inhibited by UDI  
 302 (Kaufmann et al. 2007[21]; Kishtawal et al. 2010[22]).



303  
 304 Fig. 5 Average annual summer rainfall of urban and rural stations in five climate regions. LR is shown on the  
 305 left, and HR is shown on the right

306 **2.2 Reasons for urban-rural precipitation differences**

307 **2.2.1 Relative dependence of precipitation on convective unstable energy and humidity**

308 According to the analysis in the prior section (2.1.2), afternoon (12:00-18:00) may be the period  
 309 when the UHI has the strongest influence on convective precipitation. During this period, both the height  
 310 and turbulence intensity of the boundary layer are the largest and the atmospheric state is unstable.  
 311 Therefore, it is beneficial to trigger or strengthen the development of convective motion (Baik et al.  
 312 2007[3]). Because the highest temperature and lowest RH occur in the daytime (picture omitted),  
 313 convective precipitation may be simultaneously promoted by high temperature and suppressed by low  
 314 humidity. Studying precipitation during this period may provide insights on the dominant factors  
 315 affecting convective precipitation. Considering that the LR peak mainly occurs at night (00:00-06:00) in  
 316 all regions (Fig. 4c, 4d) (although the LR peak also occurs in the afternoon (12:00-18:00), it is not obvious  
 317 in this period in the MUYR and NCP), Fig. 6c, 6d extracts LR of nighttime period (00:00-6:00). In this  
 318 study, we used the long-term observation precipitation data which limited us to specifically separate  
 319 convective cloud precipitation and stratiform cloud precipitation. According to the high intensity  
 320 characteristic of convective cloud precipitation and the short time, and long duration characteristics of  
 321 stratiform cloud precipitation, it is believed that LR mainly reflects the characteristics of stratiform cloud  
 322 precipitation while HR mainly reflects the characteristics of convective cloud precipitation.

323 The CAPE is mainly used to characterize the unstable energy of the atmosphere. Convective  
 324 precipitation may increase with the increase of atmospheric convective instability (Lepore et al.  
 325 2015[23]). The CAPE and water vapor content of the whole layer in the PRD and YRD are higher than  
 326 that in the MUYR, NCP and NEC, while the dew-point deficit in the PRD and YRD is smaller than that  
 327 in the MUYR, NCP and NEC. This finding indicates that the PRD and YRD have more convective energy

328 and are more moist within the low layers (CAPE>600 J/kg at 14:00 LT and water vapor content >45  
329 kg/m<sup>2</sup> at 14:00 LT in the PRD and YRD, CAPE≤500 J/kg and water vapor content≤40 kg/m<sup>2</sup> at 14:00  
330 LT in the MUYR, NCP, and NEC). The dew-point deficit and the water vapor content of whole layer can  
331 be used to characterize the humidity of the atmosphere. A small dew-point deficit and large water vapor  
332 content are indicative of a moist atmosphere and favorable for precipitation. Fig. 6a, 6b, and 6d show  
333 that precipitation is positively correlated with the water vapor content and CAPE of entire layers, while  
334 regions of a larger CAPE tend to have higher humidity. Dong et al. (2019)[7] found that the impacts of  
335 the CAPE and atmospheric precipitable water on precipitation showed the opposite correlations in  
336 various regions. Their results showed that the efficiency of water vapor conversion to precipitation is  
337 higher in dry climates over northern China than in wet climates over southern China, which means that  
338 in the dry climates of northern China, precipitation is mainly related to the water vapor content. In  
339 contrast, the efficiency of CAPE conversion into the airflow rising speed of atmospheric vertical motion  
340 is higher in humid climates over southern China, which means that in humid climates of southern China,  
341 precipitation is mainly related to the CAPE.

342 The relative dependence of precipitation on the CAPE and humidity can be summarized via the  
343 following regression equation:

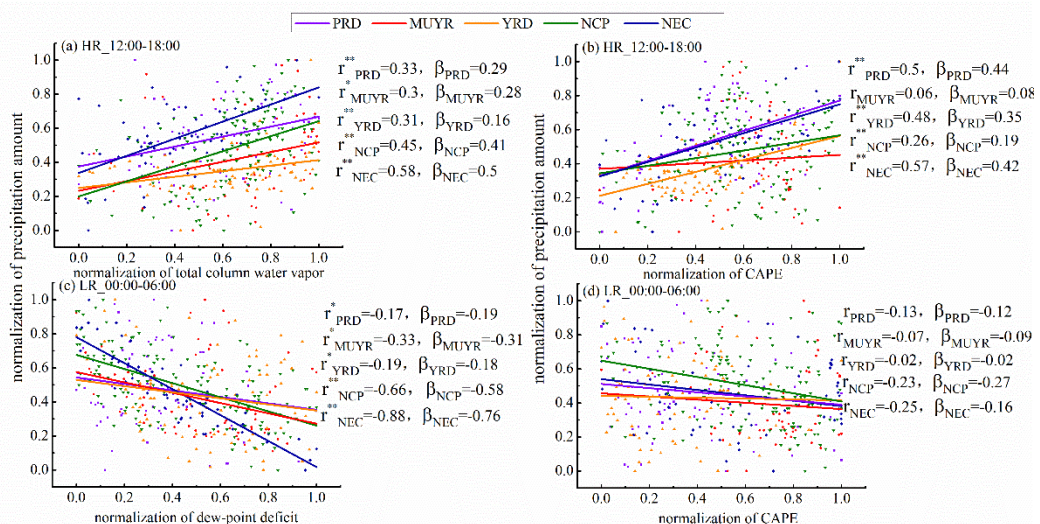
344  $y = \beta x + \text{constant}$  (2),

345 where  $y$  is the HR or LR;  $x$  is the CAPE, water vapor content of the whole layer, or 2 m dew-point deficit;  
346 and  $\beta$  represents the efficiency of  $x$  being converted to  $y$ . In Fig. 6,  $r$  represents the degree of fitting, and  
347  $r$  values closer to 1 indicate a higher fitting correlation. To directly compare the value of  $\beta$ , all physical  
348 quantities in Fig. 6 have been normalized.

349 In the PRD and YRD, the conversion efficiency of the CAPE to HR ( $\beta_{\text{PRD}}=0.44$ ,  $\beta_{\text{YRD}}=0.35$  in Fig.  
350 6b) is higher than the conversion efficiency of water vapor content to HR ( $\beta_{\text{PRD}}=0.29$ ,  $\beta_{\text{YRD}}=0.16$  in Fig.  
351 6a). In contrast, in the MUYR, NCP and NEC, the efficiency of converting water vapor content into HR  
352 ( $\beta_{\text{MUYR}}=0.28$ ,  $\beta_{\text{NCP}}=0.41$ ,  $\beta_{\text{NEC}}=0.5$  in Fig. 6a) is higher than the efficiency of converting CAPE into HR  
353 ( $\beta_{\text{MUYR}}=0.08$ ,  $\beta_{\text{NCP}}=0.19$ ,  $\beta_{\text{NEC}}=0.42$  in Fig. 6). A statistical analysis indicated that the HR in the PRD and  
354 YRD may mainly affected by the conversion of the CAPE into the airflow rising speed of atmospheric  
355 vertical motion, which means that the HR differences between urban and rural areas may be greatly  
356 affected by the UHI, and causes more urban HR. Nevertheless, the HR in the MUYR, NCP, and NEC  
357 may be more affected by the efficiency of converting water vapor into cloud droplets and raindrops,  
358 which signifies that the HR differences between urban and rural areas may be greatly affected by UDI.  
359 Urban evaporation decreases and temperature increases, which results in lower humidity and HR over  
360 urban areas than rural areas. As the HR of the MUYR, NCP, and NEC is mainly affected by the water  
361 vapor content, HR may be greatly inhibited by the UDI in these regions. However, the HR of the PRD  
362 and YRD is mainly affected by the CAPE, where the UHI may greatly promote urban HR. The above  
363 results are also consistent with the positive HR differences between urban and rural areas in the PRD and  
364 YRD and the negative HR differences in the MUYR, NCP, and NEC (Fig. 5). Except for the MUYR, the  
365 HR in all regions passed the 99% significance test. In the MUYR, the relationship between HR and water  
366 vapor content passed the 98% significance test (Fig. 6b, 6d). Considering the high altitude of the Sichuan-  
367 Chongqing region (close to the MUYR), which has an undulating terrain and is close to the Qinghai-  
368 Tibet Plateau, HR is affected by other factors, which may weaken the influence of the CAPE on HR  
369 (Liang et al. 2013[29]). A previous study showed that based on the unique topography, summer rainfalls  
370 over the MUYR (especially Sichuan) are often triggered by sub-synoptic scale cyclones near the  
371 southeastern TP (Tibet Plateau) (so called the “Southwest Vortex” by Chinese meteorologists), troughs

372 in the westerlies, shear lines, and fronts over East Asia (Jiao et al. 2005[20]). Other researchers proposed  
 373 that the MUYR rainfalls may have directly originated from the TP (Jiang and Fan 2002[18]). Some  
 374 scholars think (Mote et al. 2007[32]) that only when other weather systems are relatively weak, the heat  
 375 island circulation plays a dominant role in local weather or climate by changing the boundary layer  
 376 structure, which then leads to an obvious impact on precipitation. Therefore, in the MUYR, the UHI  
 377 effect on precipitation may be obscured by the influence of other weather systems, resulting in a very  
 378 small correlation between precipitation and the CAPE ( $r$  values in Fig. 6b, 6d). The results of Guo et al.  
 379 (2009)[10] also showed that the summer precipitation of the MUYR had a significant positive correlation  
 380 with the precipitable water vapor, although the correlation between precipitation and local temperature  
 381 was not obvious.

382 The efficiency of converting water vapor content into LR in all regions ( $\beta_{\text{PRD}}=-0.19$ ,  $\beta_{\text{MUYR}}=-0.31$ ,  
 383  $\beta_{\text{YRD}}=-0.18$ ,  $\beta_{\text{NCP}}=-0.58$ ,  $\beta_{\text{NEC}}=-0.76$ ) is higher than the conversion efficiency of CAPE ( $\beta_{\text{PRD}}=-0.12$ ,  
 384  $\beta_{\text{MUYR}}=-0.09$ ,  $\beta_{\text{YRD}}=-0.02$ ,  $\beta_{\text{NCP}}=-0.27$ ,  $\beta_{\text{NEC}}=-0.16$ ) (Fig. 6d), indicating that LR is mainly affected by  
 385 humidity and inhibited by the UDI, which is consistent with the results that less LR occurs over urban  
 386 areas than rural areas (Fig. 5). The correlation of LR and dew-point deficit in all regions passed the 98%  
 387 significance test, although the correlation between LR and the CAPE in most regions was nonsignificant,  
 388 indicating that LR is mainly related to regional humidity and less affected by convective unstable energy.



389  
 390 Fig. 6 Relationships among the CAPE, water vapor content of the whole layer, 2 m dew-point deficit and  
 391 precipitation in different regions during the summers from 1983-2012. (a) Relationship between HR from 12:00-  
 392 18:00 and water vapor content at 14:00; (b) relationship between HR from 12:00-18:00 and CAPE at 14:00; (c)  
 393 relationship between LR from 00:00-06:00 and 2 m dew-point deficit at 02:00; and (d) relationship between LR  
 394 from 00:00-06:00 and CAPE at 02:00.  $r$  is the correlation coefficient,  $a$  is the slope, and each physical quantity has  
 395 been normalized. \*\* Indicates that the value passed the 99% significance test, and \* indicates that the value passed  
 396 the 98% significance test

### 397 2.2.2 Relative dependence of urban-rural precipitation differences on the UHI and UDI

398 The previous sections indicated that the urbanization effects on HR are inconsistent over different  
 399 climate regions. Some regions are mainly affected by the CAPE (related to the UHI), while others are  
 400 greatly affected by humidity. Cities generally show higher temperature and lower humidity than rural  
 401 areas, which means that  $\Delta T > 0$  and  $\Delta RH < 0$ .  $\Delta T$  and  $\Delta RH$  usually have opposite effects on urban HR.

402 The relative dependence of urban-rural precipitation differences on the UHI and UDI can be

403 summarized with a regression equation:

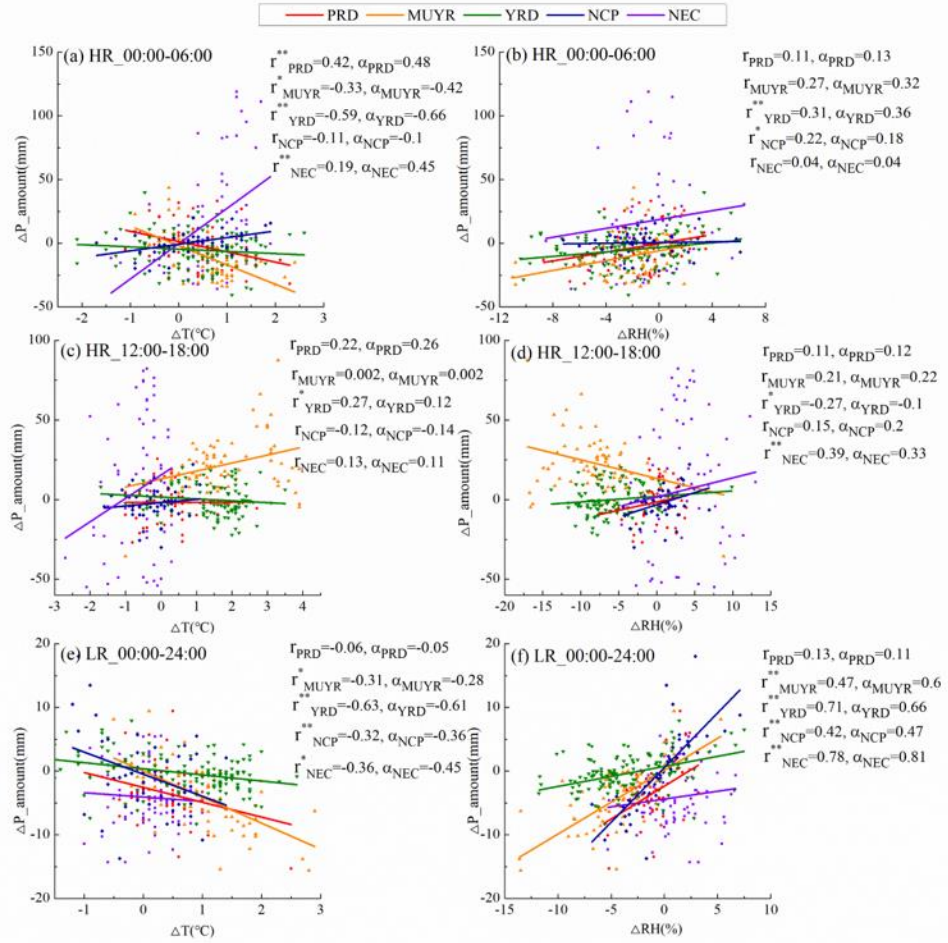
404  $\Delta y = \alpha \Delta z + \text{constant}$  (3)

405 where  $\Delta y$  is the HR or LR difference between urban and rural areas,  $\Delta z$  is the  $\Delta T$  (UHI intensity) or  
406  $\Delta RH$  (UDI intensity), and  $\alpha$  represents the efficiency of  $\Delta z$  to  $\Delta y$ . To directly compare the value of  $\alpha$ ,  
407 all physical quantities in equation (3) have been normalized.

408 The HR is more sensitive to CAPE in the PRD and YRD, where the water vapor condition is  
409 sufficient, and the UHI has greater effects on HR differences between urban and rural areas ( $\alpha_{\text{PRD}}$  in Fig.  
410 7a, 7c  $>\alpha_{\text{PRD}}$  in Fig. 7b, 7d, respectively). Hence, in polluted cities, strong atmospheric upward motion  
411 can transport aerosols to the upper air and then increase the numbers of CCNs, which helps enhance the  
412 conversion efficiency of cloud droplets to raindrops and precipitation when water vapor is sufficient  
413 (Choi et al. 2008[6]). Therefore, the PRD and YRD appears as "urban rain islands" for HR (Fig. 5). It is  
414 worth mentioning that the PRD has higher precipitation than other regions (Fig. 1a), which shows a  
415 negative difference in temperature and positive difference in humidity between urban and rural areas in  
416 the afternoon (Fig. 7c, 7d). These differences may be related to the cooling and humidification caused  
417 by precipitation itself and the moisture brought by sea breezes from coastal maritime zones. Due to heat  
418 island circulation, the urban humidification effect is more pronounced (Han et al. 2014[13]). However,  
419 cities in the YRD show significant states of "warm and dry" ( $\Delta T > 0$ ,  $\Delta RH < 0$  in Fig. 7a-f), and the  
420 promotion effect of the UHI on urban HR is stronger than the inhibition effect of the UDI on urban HR  
421 ( $\alpha_{\text{YRD}}$  in Fig. 7a, 7c  $>\alpha_{\text{YRD}}$  in Fig. 7b, 7d, respectively). In addition, due to the strong negative correlation  
422 between  $\Delta T$  and  $\Delta RH$  in the YRD (the correlation coefficient is -0.88 and passed the 99% significance  
423 test), the UDI shows a negative effect on HR in the afternoon (12:00-18:00) (Fig. 7d), which means that  
424 the combined impacts of the UHI and UDI on HR may be nonlinear. For the MUYR, NCP, and NEC,  
425 HR is more sensitive to humidity, especially in the afternoon (12:00-18:00), indicating that the UDI has  
426 a greater inhibitory effect on HR than the promotion effect of the UHI on HR ( $\alpha_{\text{MUYR}}$ ,  $\alpha_{\text{NCP}}$ ,  $\alpha_{\text{NEC}}$  in Fig.  
427 7c  $>\alpha_{\text{MUYR}}$ ,  $\alpha_{\text{NCP}}$ ,  $\alpha_{\text{NEC}}$  in Fig. 7d, respectively). Generally, UDI results in reductions in urban HR by  
428 lowering the conversion efficiency to precipitation when water vapor is insufficient. In the MUYR and  
429 NCP (where  $\Delta T > 0$  and  $\Delta RH < 0$  in Fig. 7a-f), HR is greatly suppressed by humidity shortages, which  
430 means that a greater UDI intensity corresponds to lower urban HR (Fig. 7b, 7d). However, the negative  
431 HR differences between urban and rural areas in NEC mostly occur in the afternoon (12:00-18:00) (Fig.  
432 7a-d), where the inhibitory effect of the UDI on HR is the strongest in the five climate regions ( $\alpha_{\text{NEC}}$  in  
433 Fig. 7d  $>\alpha_{\text{NEC}}$  in Fig. 7c). The differences between the YRD and NCP were partially confirmed by Zhao  
434 et al. (2019)[53], whose study supported that  $Q_1$  (atmospheric heat source, which reflects local heat  
435 sources) in the YRD was greater than that in the NCP, which is more obvious during the daytime.  $Q_2$   
436 (water vapor sink, reflecting local evaporation conditions) in the YRD was larger than that in the NCP,  
437 which was more obvious at night. Their results showed that the intensity of the UHI in the YRD was  
438 greater than that in the NCP during the daytime and less than that in the NCP at night, which indicated  
439 that the YRD has more thermal energy than the NCP and more water vapor and a stronger UHI effect  
440 during the daytime. Therefore, the YRD is more prone to convective movement during the daytime, and  
441 the strong UHI effect will further promote the occurrences of urban HR. However, the NCP has less  
442 thermal energy and water vapor and shows weak convective movement and UHI effects during the  
443 daytime; moreover, urban HR is weakly promoted by the UHI and may mainly suppressed by the UDI.

444 LR is mainly inhibited by the UDI in the five climate regions, which resulted in more LR over rural  
445 areas than urban areas. The combined effects of the UHI and UDI make the urban areas drier, which  
446 increases the likelihood of small raindrops evaporating in urban areas. On the other hand, the higher

447 temperature of the urban boundary layer increases the height of the urban water vapor condensation layer  
 448 and zero-degree layer as well as the cloud base height and the raindrop path, ultimately increasing the  
 449 possibility of small raindrop evaporation (Kaufmann et al. 2007[21]). As  $\Delta T$  becomes large, the  
 450 corresponding  $\Delta RH$  becomes small (negative value), and both effects lead to less LR in urban areas than  
 451 rural areas (Fig. 7e-f). The effects of the UDI on LR is higher than that of the UHI in all regions ( $\alpha$  in  
 452 Fig. 7f> $\alpha$  in Fig. 7e), indicating that LR is still mainly suppressed by UDI.



453

454 Fig. 7 Relationship between urban-rural precipitation differences and the UHI and UDI in various regions.  
 455 The relationship between (a) HR urban-rural differences from 00:00-06:00 and UHI at 02:00, (b) HR urban-rural  
 456 differences from 00:00-06:00 and UDI at 02:00, (c) HR urban-rural differences from 12:00-18:00 and UHI at  
 457 14:00, (d) HR urban-rural differences from 12:00-18:00 and UDI at 14:00, (e) LR urban-rural differences for all  
 458 day and diurnal average UDI, and (f) LR urban-rural differences for all day and diurnal average UHI.  $r$  represents  
 459 the fitting coefficient,  $\alpha$  is the normalized slope, \*\* indicates that the value passed the 99% significance test, and \*  
 460 indicates that the value passed the 98% significance test

### 461 3 Conclusions

462 This study uses 30-year (1983-2012) summer meteorological observational data and ECMWF  
 463 reanalysis data to reveal the precipitation differences between urban and rural areas. The precipitation is  
 464 divided into two categories based on intensity (HR and LR), and the study regions include five different  
 465 climate regions (PRD, MUYR, YRD, NCP, and NEC) in central and eastern China. The relative  
 466 dependence of precipitation on meteorological factors (UHI, UDI, CAPE, water vapor content in the

467 whole atmospheric layer, and dew-point deficit) is analyzed, which explains the inconsistent urbanization  
468 effects on precipitation over different typical climate regions. The main conclusions are as follows.

469 (1) Urbanization shows inconsistent effects on precipitation at different intensities and in different  
470 climate regions. LR is greater over rural areas than urban areas. HR is higher over the urban  
471 areas of the PRD and YRD than rural areas, while HR is lower over the urban areas of the  
472 MUYR, NCP and NEC than rural areas. This phenomenon is similar to trends found for the  
473 precipitation amounts, precipitation counts, and precipitation durations.

474 (2) There are no obvious differences between urban and rural areas in precipitation diurnal  
475 variations, although the afternoon peak of HR in urban areas is slightly earlier than that in rural  
476 areas, which may be related to the ability of the UHI to trigger precipitation formation  
477 conditions faster.

478 (3) The inconsistent effects of urbanization on HR in different climate regions can be explained  
479 by the relative dependence of precipitation on the CAPE and humidity in various climate  
480 regions. The HR is greatly affected by the CAPE in the PRD and YRD ( $\beta_{PRD}=0.44$ ,  $\beta_{YRD}=0.35$   
481 in Fig. 6b  $>\beta_{PRD}=0.29$ ,  $\beta_{YRD}=0.16$  in Fig. 6a), where convective movements are strong and  
482 water vapor are abundant (CAPE  $>600$  J/kg at 14:00 LT and water vapor content  $>45$  kg/m<sup>2</sup> at  
483 14:00 LT). Therefore, higher HR occurs in urban areas because of the UHI. In contrast, the HR  
484 is greatly affected by humidity in the MUYR, NCP, and NEC ( $\beta_{MUYR}=0.28$ ,  $\beta_{NCP}=0.41$ ,  
485  $\beta_{NEC}=0.5$  in Fig. 6a  $>\beta_{MUYR}=0.08$ ,  $\beta_{NCP}=0.19$ ,  $\beta_{NEC}=0.42$  in Fig. 6b), where the water vapor  
486 contents and convective instability energy are less (CAPE  $\leq 500$  J/kg and water vapor  
487 content  $\leq 40$  kg/m<sup>2</sup> at 14:00 LT) and the UDI impacts suppress HR in urban areas. Finally, the  
488 LR has a good correlation with humidity in all regions, which means that LR is mainly affected  
489 by the suppression impacts of the UDI and less LR is seen in urban areas than rural areas.

490 The results of this study indicate that urbanization promotes HR in wet climates (PRD and YRD),  
491 suppresses HR in dry climates (MUYR, NCP and NEC), and suppresses LR in all regions of central and  
492 eastern China during summer. Since the physical mechanism underlying the above conclusions are based  
493 on statistical analyses and the results of other researchers' literature, a deeper investigation needs to be  
494 carried out with the help of future model analyses.

495 **Acknowledgments:** This work is supported by the National Key Research and Development Program  
496 of China (2016YFA0602003)  
497 and the National Natural Science Foundation of China (Grant No. 41575148).

## 498 References

499 [1] Baik JJ (1992) Response of a stably stratified atmosphere to low-level heating an application  
500 to the heat island problem. *Journal of Applied Meteorology* 31:291-303

501 [2] Baik JJ, Kim YH, Chun HY (2001) Dry and moist convection forced by an urban heat island.  
502 *J Appl Meteor* 40:1462-1475

503 [3] Baik JJ, Kim YH, Kim JJ et al (2007) Effects of boundary-layer stability on urban heat island-  
504 induced circulation. *Theoretical and Applied Climatology* 89:73-81

505 [4] Bornstein R, Lin Q (2000) Urban heat islands and summertime convective thunderstorms in  
506 Atlanta: Three case studies. *Atmospheric Environment* 34:507-516

507 [5] Changnon SA (1979) Rainfall Changes in Summer Caused by St. Louis. *Science* 205:402-404

508 [6] Choi YS, Ho CH, Kim J, Gong DY, Park RJ (2008) The impacts of aerosols on the summer  
509 rainfall frequency in China. *J Appl Meteor Climatol* 47:1802-1813

510 [7] Dong WH, Lin YL, Wright JS et al (2019) Precipitable water and CAPE dependence of rainfall  
511 intensities in China. *Climate Dynamics* 52:3357-3368

512 [8] Guo JX (2014a) Research on Environmental Standards for Surface Meteorological Elements  
513 Observation (in Chinese). *China Science and Technology Achievements* 15:30-32

514 [9] Guo X, Fu D et al (2014b) A case study of aerosol impacts on summer convective clouds and  
515 precipitation over northern China. *Atmospheric Research* 142:142-157

516 [10] Guo J, Li GP (2009) Climatic Characteristics of Precipitable Water Vapor and Relations to  
517 Surface Water Vapor Column in Sichuan and Chongqing Region (in Chinese). *Journal of*  
518 *Natural Resources* 24:344-350

519 [11] Guo T, Zhu B, Kang Z, Gui H, Kang H (2016) Spatial and temporal distribution characteristic  
520 of fog days and haze days from 1960–2012 and impact factors over the Yangtze River Delta  
521 Region (in Chinese). *China Environmental Science* 36:961-969

522 [12] Han JY, Baik JJ (2008) A theoretical and numerical study of urban heat island-induced  
523 circulation and convection. *J Atmos Sci* 65:1859-1877

524 [13] Han JY, Baik JJ, Lee H (2014) Urban impacts on precipitation. *Asia-Pacific Journal of*  
525 *Atmospheric Sciences* 50:17-30

526 [14] Hao Z, Aghakouchak A, Phillips TJ (2013) Changes in concurrent monthly precipitation and  
527 temperature extremes. *Environ Res Lett* 8:1402-1416

528 [15] He LQ, Yang P, Jing X et al (2017) Analysis of temporal-spatial variation of heat island effect  
529 in Pearl River Delta using MODIS images and impermeable surface area. *Remote Sensing for*  
530 *Land and Resources* 29:140-146

531 [16] Houze RA (1993) *Cloud Dynamics*. Academic Press, New York

532 [17] Hua L, Ma Z, Guo W (2008) The impact of urbanization on air temperature across China.  
533 *Theoretical and Applied Climatology* 93:179-194

534 [18] Jiang JX, Fan MZ (2002) Convective clouds and mesoscale convective systems over the  
535 Tibetan Plateau in summer (in Chinese). *Chin J Atmos Sci* 26:263–270

536 [19] Jiang ZH, Li Y, Huang DL (2016) Impact of urbanization in different regions of eastern china  
537 on precipitation and its uncertainty. *Journal of Tropical Meteorology* 461:382-392

538 [20] Jiao MY, Li C, Li YX (2005) Mesoscale analyses of a Sichuan heavy rainfall (in Chinese). *J*  
539 *Appl Meteor Sci* 16:699-704

540 [21] Kaufmann RK, Seto KC, Schneider A et al (2007) Climate Response to Rapid Urban Growth:  
541 Evidence of a Human-Induced Precipitation Deficit. *Journal of Climate* 20:2299-2306

542 [22] Kishtawal CM, Niyogi D, Tewari M et al (2010) Urbanization signature in the observed heavy  
543 rainfall climatology over India. *International Journal of Climatology* 30:1908-1916

544 [23] Lepore C, Veneziano D, Molini A (2015) Temperature and CAPE dependence of rainfall  
545 extremes in the eastern United States. *Geophys Res Lett* 42:74-83

546 [24] Li WB, Chen S, Chen GX et al (2011a) Urbanization signatures in strong versus weak  
547 precipitation over the Pearl River Delta metropolitan regions of China. *Environmental*  
548 *Research Letters* 6:034020

549 [25] Li XX, Koh TY, Panda J et al (2016) Impact of urbanization patterns on the local climate of a  
550 tropical city, Singapore: an ensemble study. *Journal of Geophysical Research: Atmospheres*  
551 121:4386-4403

552 [26] Li ZQ, Niu F, Fan JW et al (2011b) Long-term impacts of aerosols on the vertical development  
553 of clouds and precipitation. *Nature Geoscience* 4:888-894

554 [27] Li ZQ, Wang Y, Guo JP, Zhao CF, Cribb MC, Dong XQ et al (2019) East Asian study of  
555 tropospheric aerosols and their impact on regional clouds, precipitation, and climate (EAST-  
556 AIR<sub>CPC</sub>). *Journal of Geophysical Research: Atmospheres* 124:13026-13054

557 [28] Liang P, Ding YH (2017) The long-term variation of extreme heavy precipitation and its link  
558 to urbanization effects in Shanghai during 1916–2014. *Adv Atmos Sci* 34:321-334

559 [29] Liang L, Li YQ, Hu HR et al (2013) Numerical simulation of the relationship between summer  
560 susceptibility anomalies on the Qinghai-Tibet Plateau and precipitation in Sichuan and  
561 Chongqing areas (in Chinese). *Plateau Meteorology* 32:1538-1545

562 [30] Lin CY, Chen WC, Chang PL et al (2011) Impact of the urban heat island effect on precipitation  
563 over a complex geographic environment in Northern Taiwan. *Journal of Applied Meteorology*  
564 and Climatology 50:339-353

565 [31] Miao S, Chen F, Li Q et al (2011) Impacts of Urban Processes and Urbanization on Summer  
566 Precipitation: A Case Study of Heavy Rainfall in Beijing on 1 August 2006. *Journal of Applied*  
567 *Meteorology and Climatology* 50:806-825

568 [32] Mote TL, Lacke MC, Shepherd JM (2007) Radar signatures of the urban effect on precipitation  
569 distribution: A case study for Atlanta, Georgia. *Geophysical Research Letters* 34:20710

570 [33] Ntelekos AA, Donner L, Fast JD, Gustafson WI, Chapman EG, Krajewski WF (2009) The  
571 effects of aerosols on intense convective precipitation in the northeastern United States. *Quart*  
572 *J Roy Meteor Soc* 135:1367-1391

573 [34] Oke TR (1973) City size and the urban heat island. *Atmos Environ* 7:769-779

574 [35] Olfe DB, Lee RL (1971) Linearized calculations of urban heat island convection effects. *J*  
575 *Atmos Sci* 28:1374-1388

576 [36] Rosenfeld D (1999) TRMM observed first direct evidence of smoke from forest fires inhibiting  
577 rainfall. *Geophys Res Lett* 26:3105-3108

578 [37] Rosenfeld D (2000) Suppression of Rain and Snow by Urban and Industrial Air Pollution.  
579 *Science* 287:1793-1796

580 [38] Rosenfeld D, Lohmann U, Raga GB et al (2008) Flood or Drought: How Do Aerosols Affect  
581 Precipitation?. *Science* 321:1309-1313

582 [39] Rozoff CM, Cotton WR, Adegoke JO (2003) Simulation of St. Louis, Missouri, land use impact  
583 on thunderstorms. *J Appl Meteor* 42:716-738

584 [40] Pruppacher HR, Klett JD (1997) *Microphysics of Clouds and Precipitation*. Kluwer Academic  
585 Publishers, Netherlands

586 [41] Shastri H, Paul S, Ghosh S, Karmakar S (2015) Impacts of urbanization on Indian summer  
587 monsoon rainfall extremes. *J Geophys Res Atmos* 120:495-516

588 [42] Shem W, Shepherd M (2009) On the impact of urbanization on summertime thunderstorms in  
589 Atlanta: two numerical model case studies. *Atmospheric research* 92:172-189

590 [43] Song X, Zhang J, Aghakouchak A et al (2014) Rapid urbanization and changes in  
591 spatiotemporal characteristics of precipitation in Beijing metropolitan area. *Journal of*  
592 *Geophysical Research: Atmospheres* 119:11250-11271

593 [44] Souma K, Tanaka K, Suetsugi T et al (2013) A comparison between the effects of artificial land  
594 cover and anthropogenic heat on a localized heavy rain event in 2008 in Zoshigaya, Tokyo,  
595 Japan. *Journal of Geophysical Research: Atmospheres* 118:11600-11610

596 [45] Tayan M, Toros H. (1997) Urbanization effects on regional climate change in the case of four  
597 large cities of Turkey. *Climatic Change* 35:501-524

598 [46] Wang J, Feng J, Yan Z (2015) Potential sensitivity of warm season precipitation to urbanization  
599 extents: Modeling study in Beijing-Tianjin-Hebei urban agglomeration in China. *J Geophys*  
600 *Res Atmos* 120:9408-9425

601 [47] Wu FB, Tang JP (2015) Impact of Urbanization on Summer Precipitation and Temperature in  
602 the Yangtze River Delta (in Chinese). *Journal of Tropical Meteorology* 31:255-263

603 [48] Yan SQ, Zhu B, Kang HQ (2019) Long-term fog variation and its impact factors over polluted  
604 regions of East China. *Journal of Geophysical Research: Atmospheres* 124:1741-1754

605 [49] Yang G, Bowling LC, Cherkauer KA, Pijanowski BC (2011) The impact of urban development  
606 on hydrologic regime from catchment to basin scales. *Landscape Urban Plan* 103:237-247

607 [50] Yang Y, Wu B, Shi C, Zhang J, Li Y, Tang W, Shi T (2013) Impacts of urbanization and station-  
608 relocation on surface air temperature series in Anhui Province, China. *Pure and Applied*  
609 *Geophysics* 170:1969-1983

610 [51] Zhang CL, Chen F, Miao SG et al (2009) Impacts of urban expansion and future green planting  
611 on summer precipitation in the Beijing metropolitan area. *Journal of Geophysical Research:*  
612 *Atmospheres* 114:356-360

613 [52] Zhang N, Gao Z, Wang X et al (2010) Modeling the impact of urbanization on the local and  
614 regional climate in Yangtze River Delta, China. *Theoretical and Applied Climatology* 102:331-  
615 342

616 [53] Zhao XT, Zhu B, Pan C (2019) Research on temperature difference of urban-rural areas in  
617 different climate in central-eastern China. *Journal of the Meteorological Sciences* 39: 569-577

618 [54] Zhou L, Jiang ZH, Li ZX et al (2015) Simulation of climate effects of underlying surface  
619 changes in different urban agglomerations in eastern China (in Chinese). *Chinese Journal of*  
620 *Atmospheric Sciences* 39:596-610